International Journal of Nanomedicine

Dovepress
open access to scientific and medical research

Open Access Full Text Article

ORIGINAL RESEARCH

Preparation of brushite cements with improved properties by adding graphene oxide

This article was published in the following Dove Press journal:
International Journal of Nanomedicine

Negar Nasrollahi[1]
Azar Nourian Dehkordi[1]
Abbas Jamshidizad[1]
Mohammad Chehelgerdi[2]

[1]Department of Stem Cell and Regenerative Medicine, Institute of Medical Biotechnology, National Institute of Genetic Engineering and Biotechnology, Tehran, Iran; [2]Biotechnology Research Center, Shahrekord Branch, Islamic Azad University, Shahrekord, Iran

Background: Brushite (dicalcium phosphate dihydrate, DCPD) cement as a promising bioactive material for bone tissue engineering is widely used to treat defects. However, relatively poor mechanical properties of brushite cement limit its application in loadbearing conditions. The aim of this study is to investigate the effect of graphene oxide (GO) addition to the physical-mechanical-biological properties of brushite cement.

Methods: The brushite types of cement were prepared by mixing β-tricalcium phosphate [β-TCP, Ca3 (PO4)2] and monocalcium phosphate monohydrate [MCPM, Ca(H2PO4)2. H2O]. GO was introduced at 0, 0.5, 2, and 5 wt.% with the liquid. MG63 cells were cultured on the GO/CPC surfaces to observe various cellular activities and hydroxyapatite (HA) mineralization.

Results: Based on our results, GO/CPC composites exhibit improvement in compressive strength compared to pure CPC. New Ca-deficient apatite layer was deposited on the composite surface after immersing immersion in SBF for 7 and 14 days. Field emission scanning electron microscope (FESEM) images indicated that pure and GO incorporated brushite cement facilitates cell adhesion. CPC/GO was slightly toxic to cells such that high concentrations of GO decreased the cell viability. Besides, alkaline phosphatase (ALP) activity of cells was improved compared with the pure CPC.

Conclusion: Our results highlight the role of graphene oxide that may have great potential in enabling the utility of graphene-based materials in various biomedical applications.

Keywords: calcium phosphate cement, graphene oxide, biocompatibility, bioactivity, mechanical properties

Introduction

Restorable calcium phosphate bone filling materials have recently received attention owing to its similarity to the bone because calcium phosphates are the most critical inorganic constituents of biological hard tissues.[1] There are significant advantages in using Calcium Phosphate Cement (CPC) since they offer the excellent biocompatibility, osteoconductivity, surgeon moldability, injectability, and complete filling of a cavity, which can stimulate bone regeneration.[2–4] Based on the final product, CPC is classified into two categories: apatite and brushite. Brushite cement is generally made by β-tricalcium phosphate [β-TCP, Ca3 (PO4)2] and monocalcium phosphate monohydrate [MCPM, Ca(H2PO4)2. H2O].[5] This cement has been recognized for its fast setting, brittleness, and low strength (approximately 15 MPa–52 MPa).[6] It is expected that this cement will overcome their problems and drawbacks. Several methods such as the addition of nanoparticles have been used to develop a strong CPC. In recent years, graphene-based nanofillers have been applied to improve the

Correspondence: Mohammad Chehelgerdi
Biotechnology Research Center, Shahrekord Branch, Islamic Azad University, Postal Box: 166, Shahrekord, Iran
Tel/Fax +98 381 336 1001
Email Chehelgerdi1992@gmail.com

submit your manuscript | www.dovepress.com
DovePress
http://doi.org/10.2147/IJN.S196666

mechanical performance of ceramics.[7] Graphene, a single layer of carbon atoms in a two-dimensional (2D) hexagonal lattice, was found to exhibit excellent biocompatibility, low toxicity, unique structural features, and exceptional mechanical properties.[8,9] Graphene oxide could be incorporated into cements to improve their biocompatibility and mechanical properties. Zhang et al reported the improvement of graphene nanosheets/hydroxyapatite composites in fracture toughness as compared to pure hydroxyapatite.[10] Mehrali et al reported that adding reduced graphene oxide to pure calcium silicate increased the hardness of the material, the elastic modulus, and the fracture toughness.[11] Liu et al tested reduced graphene oxide/gelatin composites with MC3T3-E1 cells and found a higher cellular activities such as cell adhesion, cell proliferation, and alkaline phosphatase activity compared with the graphene oxide or glass surface.[12] Li et al found that, compared with hydroxyapatite, the prepared graphene oxide-based hydroxyapatite composites had an increased elastic modulus and hardness.[13] The objectives of the present study were to determine the graphene oxide effects on mechanical and cellular properties of brushite cement. The hypothesis was that the incorporation of graphene oxide would increase not only mechanical properties but also enhance its cellular properties.

Materials and methods

Materials

Monocalcium phosphate monohydrate (MCPM) and graphite powder (<20 μm) were purchased from Sigma-Aldrich (Wisconsin, USA). Citric acid, calcium hydroxide, orthophosphoric acid, concentrated sulfuric acid (95–98 wt%), hydrochloric acid (37 wt%), potassium permanganate (KMnO4, 99.9%), Sodium nitrate (NaNO3, 99.9%), sodium hydroxide, Hydrogen peroxide (H2O2, 30%), nitric acid and ethanol were supplied from Merck (Germany). All aqueous solutions were prepared with deionized water. All the chemicals were of analytical grade and used without additional treatment.

Preparation of β-TCP

The preparation method of β-TCP was microwave irradiation. Briefly, calcium hydroxide and orthophosphoric acid were used as the starting materials. The initial Ca/P ratio was 1.51. The orthophosphoric acid solution was added dropwise to the calcium hydroxide suspension. The solution was mixed using a magnetic stirrer. The pH was adjusted to 6 with nitric acid (HNO3) and sodium hydroxide (NaOH). The solution mixture was immediately transferred to a domestic microwave oven (2.45 GHz, 800 W) and irradiated for 45 min. The white precipitation was centrifuged and dried at 90℃. In the final step, the powder was calcined at 900℃ for 1 h. The powder was confirmed to be β-TCP as characterized by using X-ray diffraction (XRD) and Fourier transform infrared spectrophotometer (FTIR). The XRD patterns were recorded with a diffractometer (Siemens, D5000-Germany) with CuKα radiation (λ=1.5406 A) over the 2Θ range of 5–50° in steps of 0.02°. The operation voltage and current were 35 kV and 25 mA, respectively. FTIR spectrum was performed using a Fourier transform infrared spectrophotometer (Nicolet Nexus-670 FTIR, Germany) to analyze the composition of CPCs after setting over a wavelength range of 4,000–400 cm^{-1} at a resolution of 4 cm^{-1}. KBr pressed pellet technique was used for the analysis.[14]

Preparation of graphene oxide

The graphite oxide powder was synthesized from graphite based on a modified Hummer Method.[15] About 1 g of natural graphite powder, 48 mL of sulfuric acid (98%), 500 mg of NaNO3, and 3 g of KMnO4 were used as the starting materials and mixed. The reaction flask was immersed in an ice bath. After the complete dissolution of gradual addition of KMnO4, the mixture was allowed to stir for 3 days. Then, 120 mL of deionized water was slowly added to the mixture while keeping the temperature at 70°C. After 1 h, the temperature was declined to 60 °C followed by adding 2.5 mL of 30% H2O2. The color of the mixture was changed to bright yellow. Then, the mixture was rested for 5 days to precipitate graphite oxide powder. The powder was repeatedly washed with dilute 1 M HCl and deionized water until a pH of 4–5 was achieved. Finally, the graphite oxide powder was obtained by 36 h freeze-drying the graphite oxide slurry. The powder was confirmed to be graphene oxide as characterized by XRD. To study the size and morphology of graphene oxide nanosheet, a dilute dispersion of GO in DCM (0.01 mg mL^{-1}) was developed on a freshly cleaved mica surface and imaged using an atomic force microscope (AFM, Nanoscope III Multimode, VEECO) in tapping mode.

Synthesis of CPC/GO composites

The brushite cement was composed of the obtained β-TCP and MCPM in a 45:55 molar ratio together with 1 wt.% disodium dihydrogen pyrophosphate (SPP, Sigma-Aldrich, 71501, batch no. 1103557, Germany). Citric acid (0.5 M)

was used as the liquid phase in an L/P of 0.22 ml/g.[16] In order to reduce the porosity by decreasing the amount of air trapped inside the paste during mixing, the mixing was performed twice for 30 s in falcon tubes, using a Cap-Vibrator (Ivoclar Vivadent, Liechtenstein). The CPC/GO composite cement was prepared by adding the obtained GO powder (0, 0.5, 2, and 5 wt.%) into the citric acid and then sonicated for 20–45 min. The CPC powders were mixed with citric acid and graphene oxide for 1 min to form a homogeneous paste.

Setting time

The cement paste was placed in a Teflon mold with a diameter of 6 mm and a height of 12 mm. Each specimen was set in a 100% relative humidity box at 37℃. Setting time of the cement was measured by the Vicat needle (ASTM C187-98). Generally, setting time is defined as the time necessary so that the needle (300 g, Φ =1 mm) does not penetrate deeper than 1 mm into the sample. The setting time value was the average of 3 measurements.

Mechanical property

After setting for 24 h at 37℃ in PBS solution, which was prepared according to British Pharmacopoeia (2.38 g L^{-1} Na2HPO4, 0.19 g L^{-1} KH2PO4 and 8 g L^{-1} NaCl), the compressive strength of composite cement with a diameter of 6 mm and a height of 12 mm was measured on dry specimens (dried at 70 ℃ overnight) at a loading rate of 1 mm/min with a SANTAM universal testing machine (STM 20).

Phase characterization of CPC/GO composites

For phase characterization, the fractured of optimum samples from the compressive strength experiments were collected and characterized using XRD and FTIR.

Ph measurements

Composite cement (Ø 6 × 12 mm^3) was placed in 40 ml of PBS at 37℃ for 24 h, after which the pH of the solutions was monitored with a pH/ion meter (METTLER TOLEDO MP 225).

Porosity

Porosity was measured using water evaporation method. The porosity of composite cement was calculated from $V_w = (MW - m_d)/\rho_w$ and $\Phi = V_w/Va$, where MW is the weight of the wet sample right after removal from the PBS, m_d is the weight of the dry sample, ρ_w is the density of PBS. (ie, 1 g/cm^3 at RT), V_w is the volume of the evaporated water, and V_a is the apparent volume (Ø 6 × 12 mm^3), which was measured using Archimedes principle on wet samples.[17]

Bioactivity in simulated body fluid (SBF)

In vitro bioactivities of the fabricated CPC/GO composites were evaluated in Simulated body fluid (SBF) prepared by the procedure described.[18] The set discs (Ø 6 × 3 mm^3) were immersed into a 1.5-times concentrated SBF solution at 37 ℃ over the course of 1 and 2 weeks, during which the 1.5 SBF solution was changed every day. The SBF solution was prepared using the method developed by Kokubo and Takadama.[18] For the evaluation of formation of bone-like apatite on the samples, they were removed after incubation of various soaking periods, rinsed in deionized water to remove SBF, and air-dried at room temperature until a constant weight was attained. The surface morphologies of the specimens were observed with HITACHI S-4160 field emission scanning electron microscope (FESEM).

In vitro biocompatibility

MG63 (human osteoblast-like osteosarcoma) cells were obtained from the National Cell Bank of Iran, Pasteur Institute (Tehran, Iran). Cell cultures were maintained in DMEM (L-glutamine) supplemented with 10% fetal bovine serum (FBS, Gibco) and 1% penicillin/streptomycin at 37 ℃ in a humidified atmosphere with 5% CO_2. Methylthiazolyldiphenyl-tetrazolium bromide (MTT) powder was purchased from Sigma-Aldrich (Wisconsin, USA). All set specimens were sterilized by autoclave for 1 h.

Cytotoxicity study with the use of the extracts

The cytotoxicity assay was performed according to the ISO 10993-5 protocol. Typically, 0.1 g of powder of set samples was incubated in 1 mL of sterilized culture medium. The media were extracted for using in cellular assays at the predefined time intervals (1, 3, and 7 days). The culture medium was kept under similar conditions as a negative control. The cytotoxicity of the extracts was determined using the MTT assay. In brief, MG63 with a density of 5×10^4 cells/well were cultured in a 24-well. On the next day, the culture medium was replaced with 100 µL of extracts supplemented with 10 µL FBS. The

medium was discarded after 24 h of incubation, followed by adding 100 µL of MTT solution (0.5 mg/mL in PBS) to each well. Following the incubation of cells for 4 h at 37 ℃, the dark blue formazan crystals were dissolved by adding 100 µL of DMSO per well. Finally, 100 µL of each sample was transferred to a 96-well ELISA plate and the absorbance was measured at 570 nm. The tests were repeated for three specimens in all samples. Eventually, the cell viability percentage was reported as the average absorbance of each extracted group divided by that of the control group.

Cell attachment

The brushite cement does not allow cell attachment without further treatment, because of the presence of an intermediate dicalcium phosphate-citrate complex formed in the cement as a result of using citric acid as the liquid phase. This prevention of cell attachment if

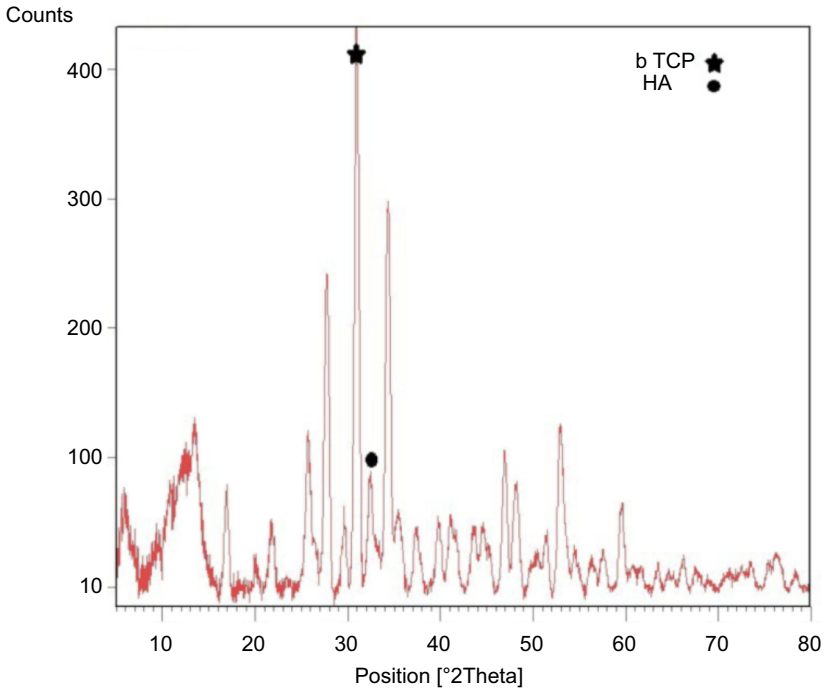

Figure 1 XRD pattern of beta-tricalcium phosphate and hydroxyapatite.
Abbreviations: XRD, X Ray Diffraction; b TCP, beta-tricalcium phosphate; HA, hydroxyapatite.

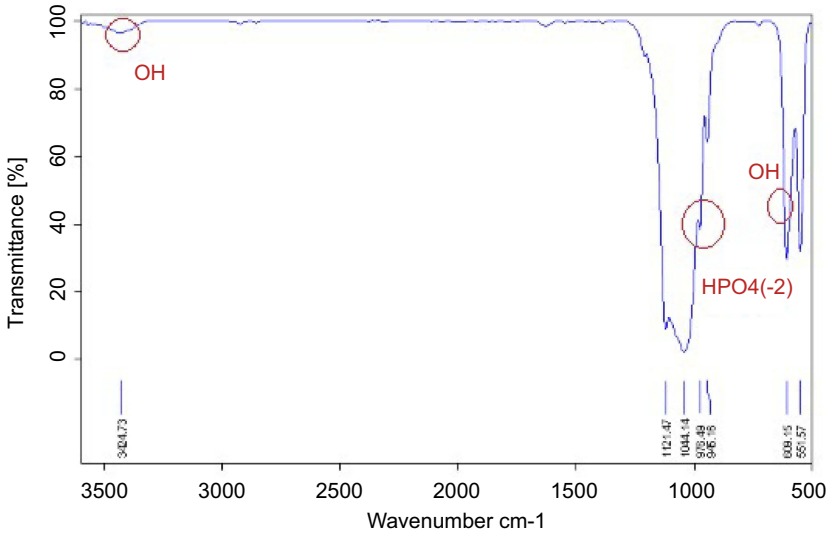

Figure 2 FTIR pattern of beta-tricalcium phosphate and hydroxyapatite.
Abbreviation: FTIR, Fourier Transform Infrared Spectroscopy.

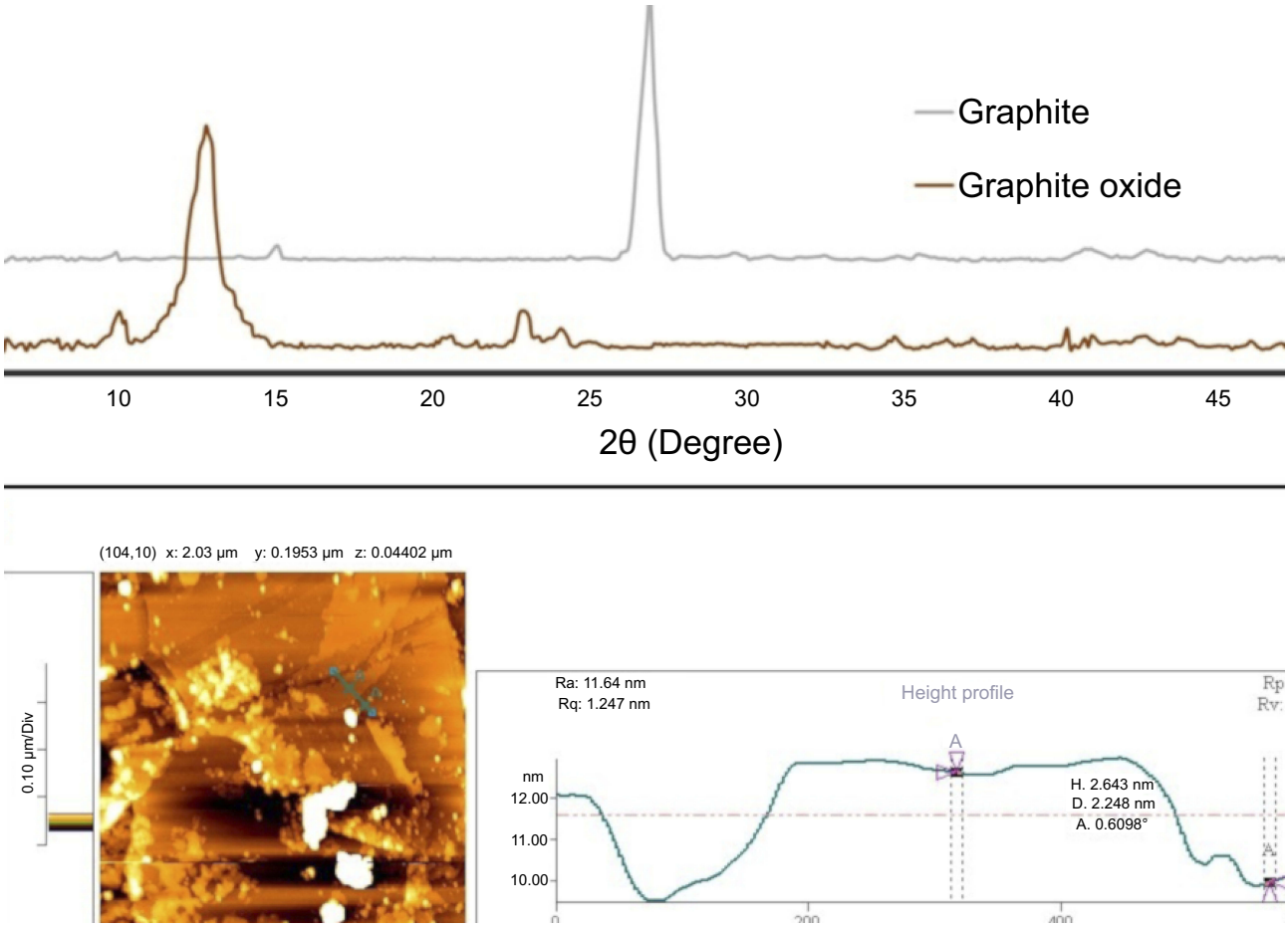

Figure 3 Structural and morphological characterization of synthesized GO: XRD (**A**) and AFM (**B**) of graphene.
Abbreviations: XRD, x-ray diffraction; AFM, Atomic Force Microscopy.

Table 1 Calcium phosphate cement setting time

Sample name	Setting time (min)
CPC	30±0.8
CPC +0.5% GO	26±1.4
CPC +2% GO	23±0.9
CPC +5% GO	17±1.0

Abbreviations: CPC, Calcium Phosphate Cement; GO, graphene oxide.

the material is implanted directly is not a significant problem.[19] Set samples (Ø 6 × 3 mm^3) were aged in serum-free DMEM at 37 ℃ over a period of 1 week. The DMEM was refreshed every 2 days. On day 7, the aged samples were seeded with MG63 under the density of 5×10^4 cells/well followed by incubation for 1 day in a humidified atmosphere of 5% CO2 at 37 ℃. At a preselected time point, the seeded sample was fixed by 2.5% (v/v) glutaraldehyde solution for 3 days followed by three washes in PBS (0.1 M). Eventually, the specimens were dehydrated in graded series of ethanol, dried in air, and sputter coated with gold-palladium prior to FESEM observation.

Alkaline phosphatase activity

MG63 additives were seeded onto CPC/GO composite specimens (Ø 3 × 6 mm^3) and were analyzed for alkaline phosphatase (ALPase) activity. ALPase assay was performed on days 3 and 7 through the conversion of a colorless p-nitrophenyl phosphate to a colored p-nitrophenol according to the manufacturer's protocol (Abcam ab83369). The absorbance at 405 nm of 4-nitrophenol was measured in a 96-well microplate reader. ALP activity was calculated from a standard curve after normalization to the total protein content. Data were expressed in nanomoles of p-nitrophenol produced per minute per microgram of protein. The tests were performed in triplicate.

Experimental data were presented as means ± standard deviation. Statistical significance was analyzed by one-way ANOVA multicomparison. ANOVA was performed

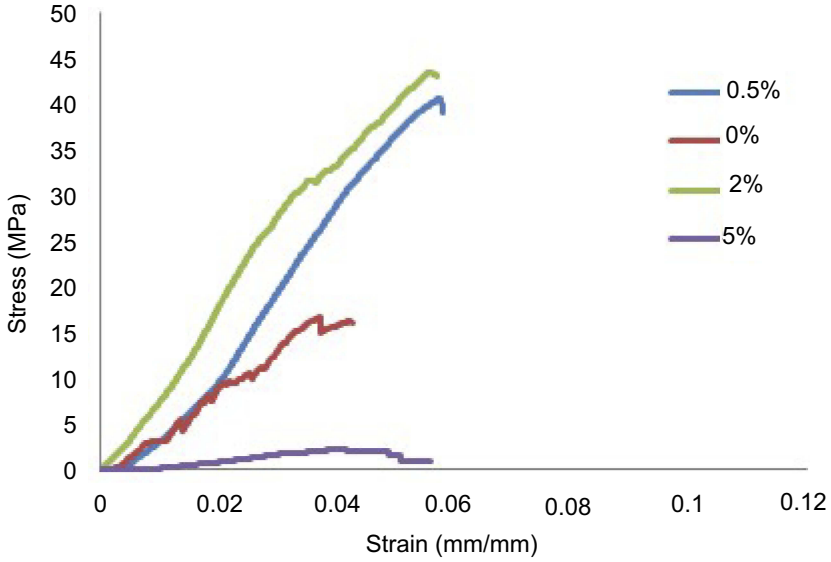

Figure 4 Stress-strain curve of composite cement.

Table 2 Compressive strength and young modulus of composite cement

CPC/ GO	Comperssion Strength (MPa)	Young Modul (GPa)
0%	12	0.4
0.5%	40	0.8
2%	42	0.8
5%	2	0.04

Abbreviations: CPC, Calcium Phosphate Cement; GO, graphene oxide.

to compare the difference in the groups. Also, the results were considered to be statistically significant at $p<0.05$ (*) or $p<0.01$ (**) with the differences between groups compared using Tukey's test.

Results and discussion

Characterization of β-TCP

The first step toward preparation of composite cement was to produce the β-TCP through a microwave irradiation method. The XRD pattern of β-TCP in Figure 1 is similar to those in other reports.[14,20] The peak was identified to be corresponding to β-TCP and indexed according to the standard value (JCPDS 09-0169). The HA peak was indexed according to the standard pattern (JCPDS 09-0432). This indicates that β-TCP was successfully synthesized, which is related to HA. To verify the formation of β-TCP the infrared spectra of the sample was measured and presented in Figure 2. The spectra illustrate the hydroxyl bond stretch at 3,550 cm^{-1} and $HOP4^{2-}$ at 970 cm^{-1} corresponding to HA and β-TCP structure, respectively. The bond of $HPO4^{2-}$ at 980 cm^{-1} shows phosphate group forming TCP. These FTIR spectra confirm the in situ formation of β-TCP.

Characterization of graphene oxide

XRD pattern in Figure 3 shows the presence of the characteristic peaks of synthesized graphite oxide. Native graphite has a peak at 2θ =26.8° corresponding to a d-spacing of 0.315 nm. In the XRD pattern of graphite oxide, the characteristic peak showed a shift to 2θ =12.9°, and the inter-layer spacing was increased to 0.798 nm. During the oxidation process, oxygen-containing groups were created on the surface of graphite sheets.[21] AFM was employed for the thickness measurements of individual and few-layered graphene oxide sheets (Figure 3). The thickness dispersion of individual graphene oxide sheet revealed that the thickness of formed nanoplatelet was about 1.5–3 nm, which is equivalent to the thickness of 2–3 layers of graphene sheets. The nanosheets displayed irregular shapes with various lateral sizes (the area on the order of 0.001 μm^2–2 μm^2).

Setting time

Table 1 shows the effects of graphene oxide incorporation in the brushite cement on the setting time. Introduction of graphene oxide resulted in a decrease in setting time. The cement paste was molded in Teflon® rings and height 5 mm, opened at both ends. The molded past was immersed in 40 ml of 37 ℃ PBS 5 min after mixing. The surface of the

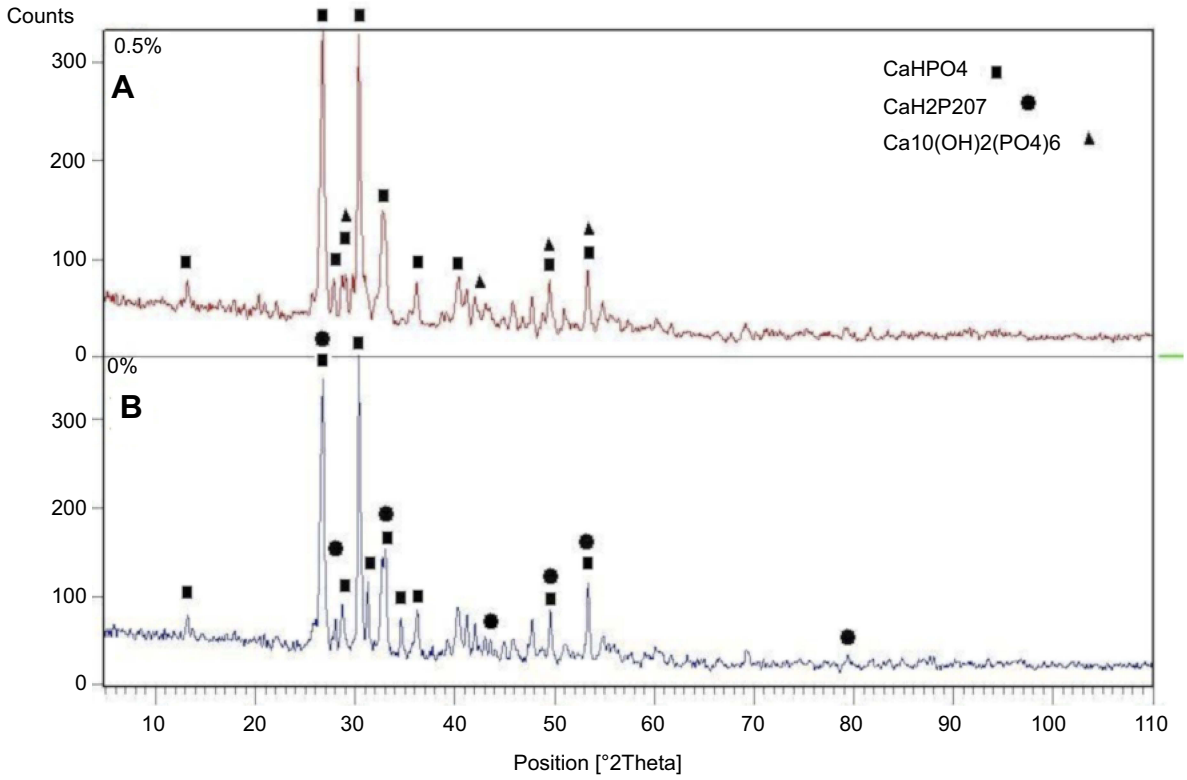

Figure 5 XRD patterns of 0.5% (**A**) and 0% (**B**) CPC/GO composite.
Abbreviations: CPC, calcium phosphate cement CPC/GO scaffold; XRD, x-ray diffraction.

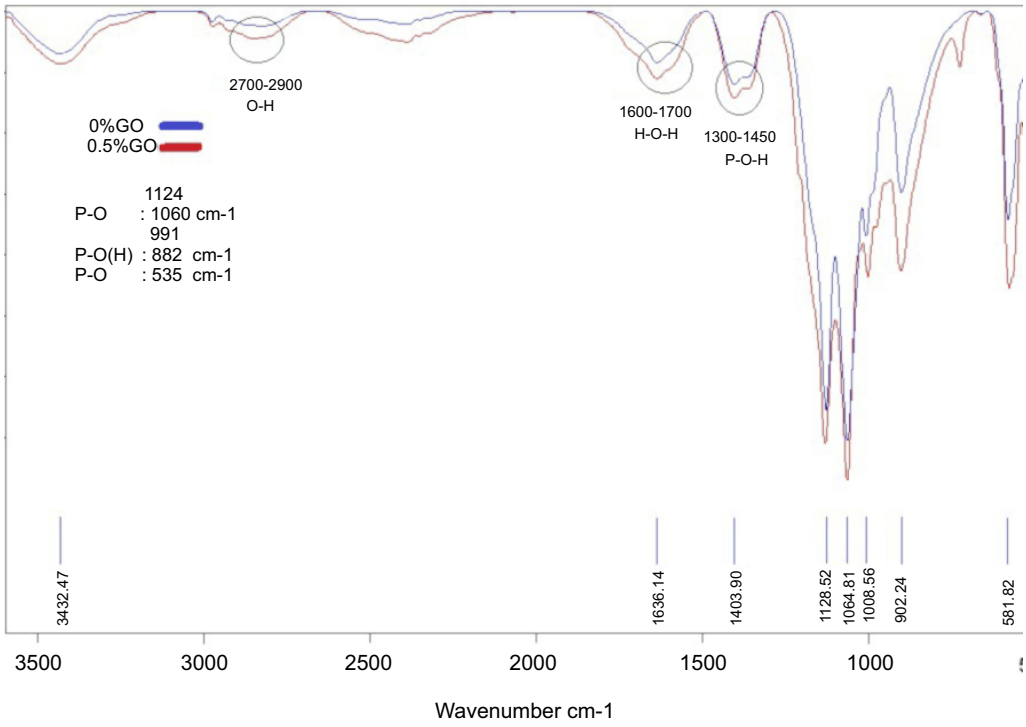

Figure 6 FTIR patterns of 0% and 0.5% CPC/GO composite.
Abbreviations: CPC, calcium phosphate cement CPC/GO scaffold; FTIR, Fourier Transform Infrared Spectroscopy.

Table 3 pH changes of cements

Sample name	pH	Solution	Time	Temperature
CPC	6.3	PBS	24 h	37 °C
CPC +0.5% GO	6.3	PBS	24 h	37 °C
CPC +2% GO	6.3	PBS	24 h	37 °C
CPC +5% GO	6.3	PBS	24 h	37 °C

Abbreviations: CPC, calcium phosphate cement CPC/GO scaffold; PBS, Phosphate buffered saline.

Table 4 Porosity of cements

Sample name	Porosity %
CPC	61
CPC +0.5% GO	61
CPC +2% GO	62
CPC +5% GO	63

Abbreviation: CPC, calcium phosphate cement CPC/GO scaffold.

cement was tested every 3 min, and the cement was considered to have set when a visible mark could not be seen on the sample after placing a 453.5 g Gillmore needle with a tip diameter of 1.06 mm (equivalent to a stress of 5 MPa) on the surface (ASTM C266-99). The time decreased from 30 min to 17 min when the weight ratio of graphene oxide varied from 0 to 5 wt.% at a P/L ratio of 0.22 ml/g.

Mechanical property

Figure 4 presents the stress-strain diagrams for CPC/GO composite samples. The compressive strength of the

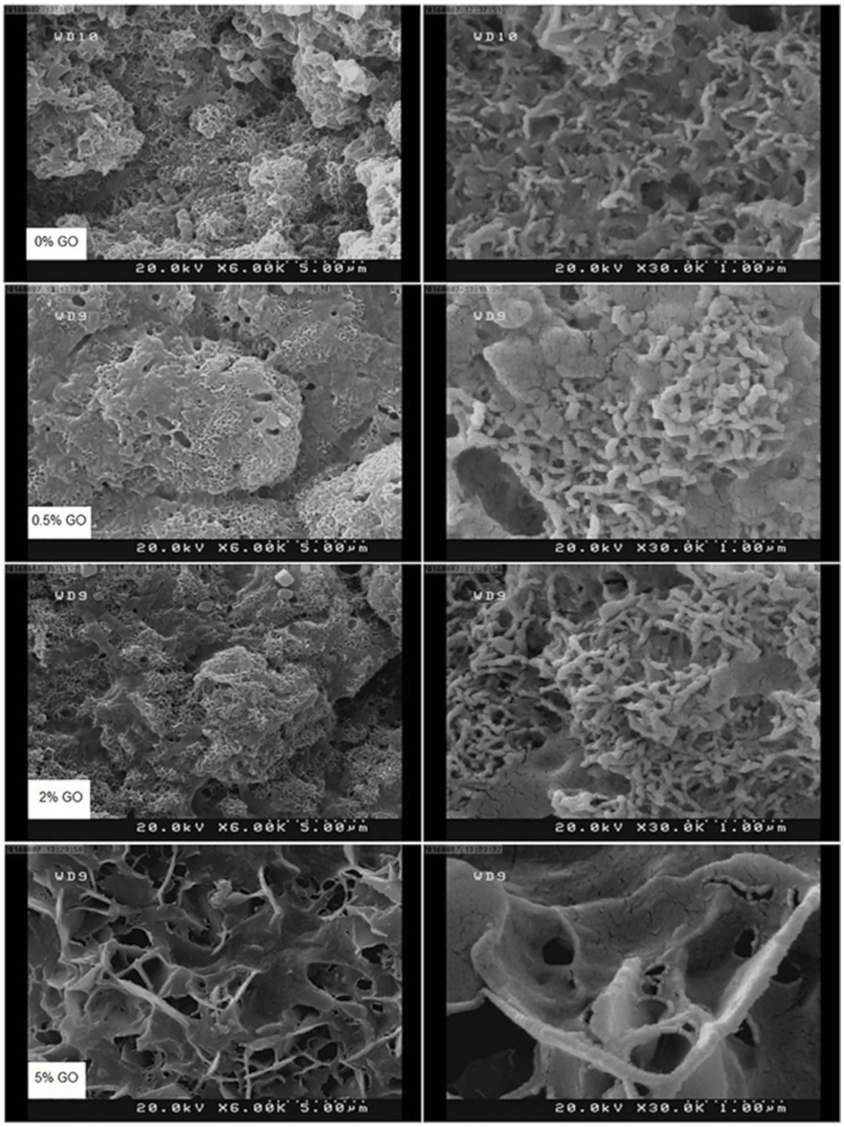

Figure 7 FESEM pictures of 0%, 0.5%, 2% and 5% cements after soaking for 7 days.
Abbreviation: FESEM, Emission scanning electron microscopy.

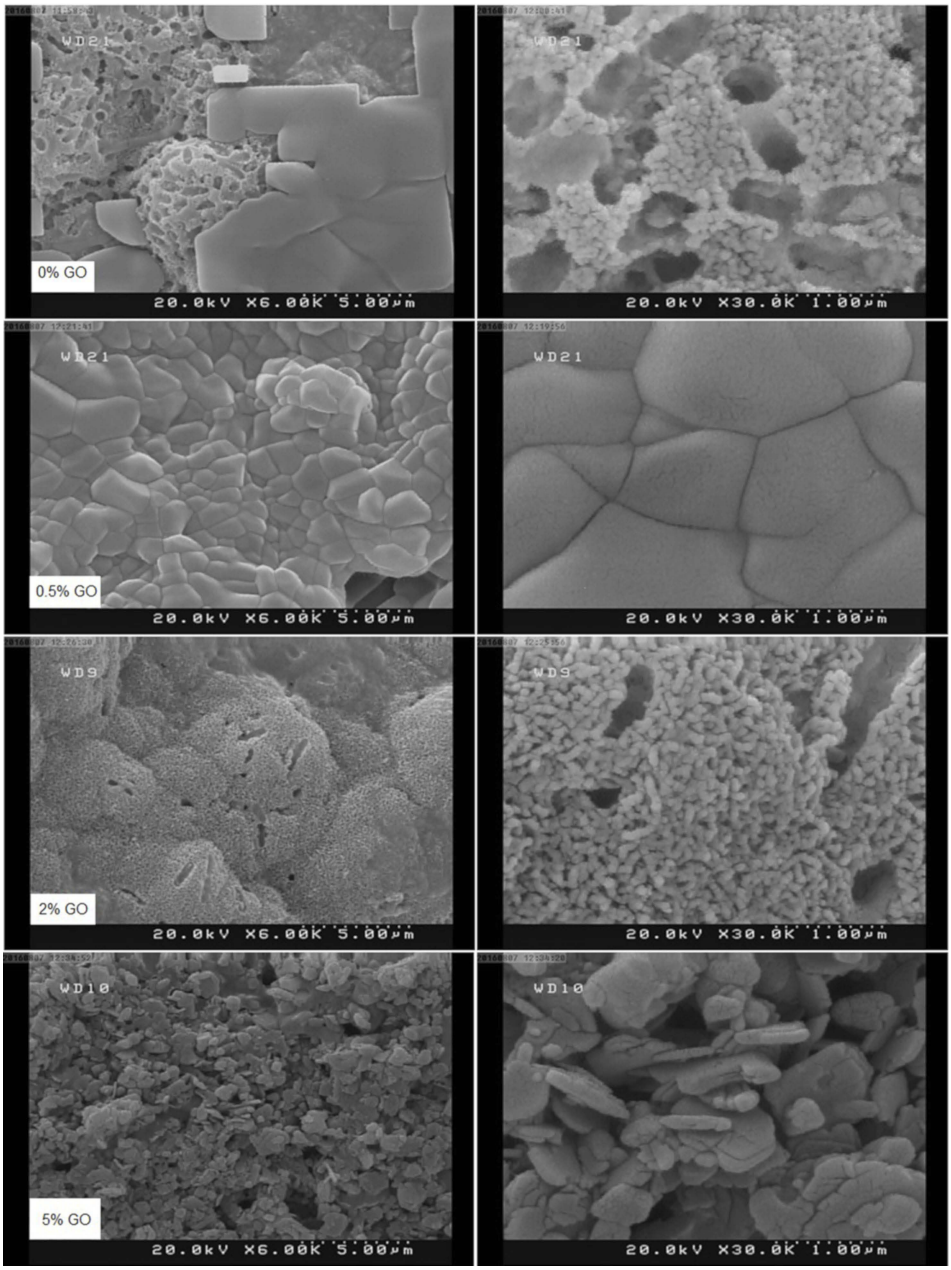

Figure 8 FESEM pictures of 0%, 0.5%, 2% and 5% cements after soaking for 14 days.
Abbreviation: FESEM, Emission scanning electron microscopy.

samples significantly increased from 12 MPa at 0% graphene oxide to 42 MPa at 2% graphene oxide. The extensive specific surface area of graphene oxide would increase the interfacial bonding in the composites and facilitate the stress transfer from the matrix to the nanofillers.[22] When 5% of graphene oxide was added, a considerable decrease was observed in strength to 2 MPa. A similar trend was also seen for elastic modulus (Table 1). The reduced compressive strength by adding 5 wt.% graphene oxide may be due to the higher number of nanoparticles present in the paste compared to the amount required to combine with the cement during the process or may be due to the defects generated in the dispersion of graphene oxide that declines the strength of the specimens (Table 2).

Phase characterization of CPC/GO composites

Figure 5 shows the XRD patterns of 0% and 0.5% CPC/GO composite samples after setting for 24 h at 37 ℃ in PBS solution. The XRD patterns for the 0% CPC/GO and 0.5% CPC/GO samples were very similar. The main peaks that corresponded to the monetite (DCPA; dicalcium phosphate

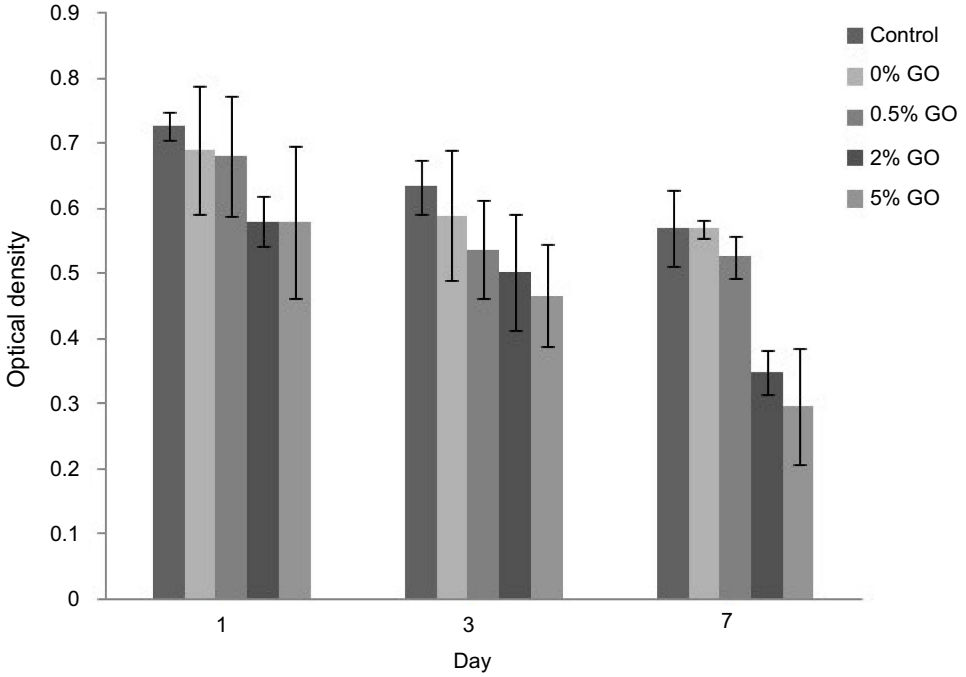

Figure 9 The cytotoxicity graph of the composite cement extract at intervals of 1, 3 and 7 days (≤0.05).

anhydrous, CaHPO4) structure were observed in both patterns at 26.4–26.6° and 30.2–30.4° (JCPDS 00-009-0080). The end product of brushite cement is brushite, and monetite can be precipitated by dehydration of brushite. The experiment showed brushite crystals transformed into monetite.[23] XRD patterns of the 0% CPC/GO indicated the presence of the characteristic peaks of calcium hydrogen diphosphate, but The XRD pattern of 0.5% GO/CPC exhibits several peaks in 2θ =20°–60°, which corresponded to the hydroxyapatite. These results indicate that the addition of graphene oxide increased the conversion to hydroxyapatite like a product. To verify the formation of monetite after setting for 24 h at 37℃ in PBS solution and the presence of graphene oxide, the infrared spectra of the samples were compared (Figure 6). The characteristic bands at 2,810, 1,633, 1,124, 1,060, 991, 882, and 535 cm^{-1} are assigned as the stretching and bending of phosphate, the stretching mode of the hydroxyl (OH) group, and the water-bending mode of monetite. Other features include the stretching vibration of the PO_4^{-3} group at approximately 535–1,124 cm^{-1}, the P-O stretching vibration at 1,000, 1,060, and 1,124 cm^{-1}, and the P-O-H in-plane bending around ~1,300–1,450 cm^{-1}. The broadband at approximately 1,636 cm^{-1} is associated with the H-O-H bending and the rotation of the residual free water. The liberation band at 2,800 cm^{-1} for the O-H stretching vibration band of HPO_4^{-2} was obtained from FTIR spectra. The 0.5% GO/CPC composite exhibits clear absorption bands resulting from the symmetric stretching of P-O-P at 726 cm^{-1}.[24] This difference may be attributed to the presence of graphene oxide or the presence of hydroxyapatite in different stoichiometric form. These results are in good agreement with the XRD analysis.

pH measurements

The pH values tended to be close to neutral pH levels after 24 h of storage in PBS (Table 3).

Porosity

For composite samples, the porosity was increased slightly, as the content of graphene oxide increased (Table 4). The slight increase in the porosity may be related to the high viscosity of pastes, which could result in a higher fraction of air bubbles that are trapped within the paste during mixing.

In vitro hydroxyapatite forming ability

After soaking for 7 and 14 days, aggregated apatite appeared on surfaces of composite specimens (Figures 7 and 8). The surfaces of the samples were observed to be covered by a denser apatite layer after immersion time from 7 to 14. When the graphene oxide concentration in the composite increased, the surface was composed of nanosheet-like apatite; however, pure calcium phosphate

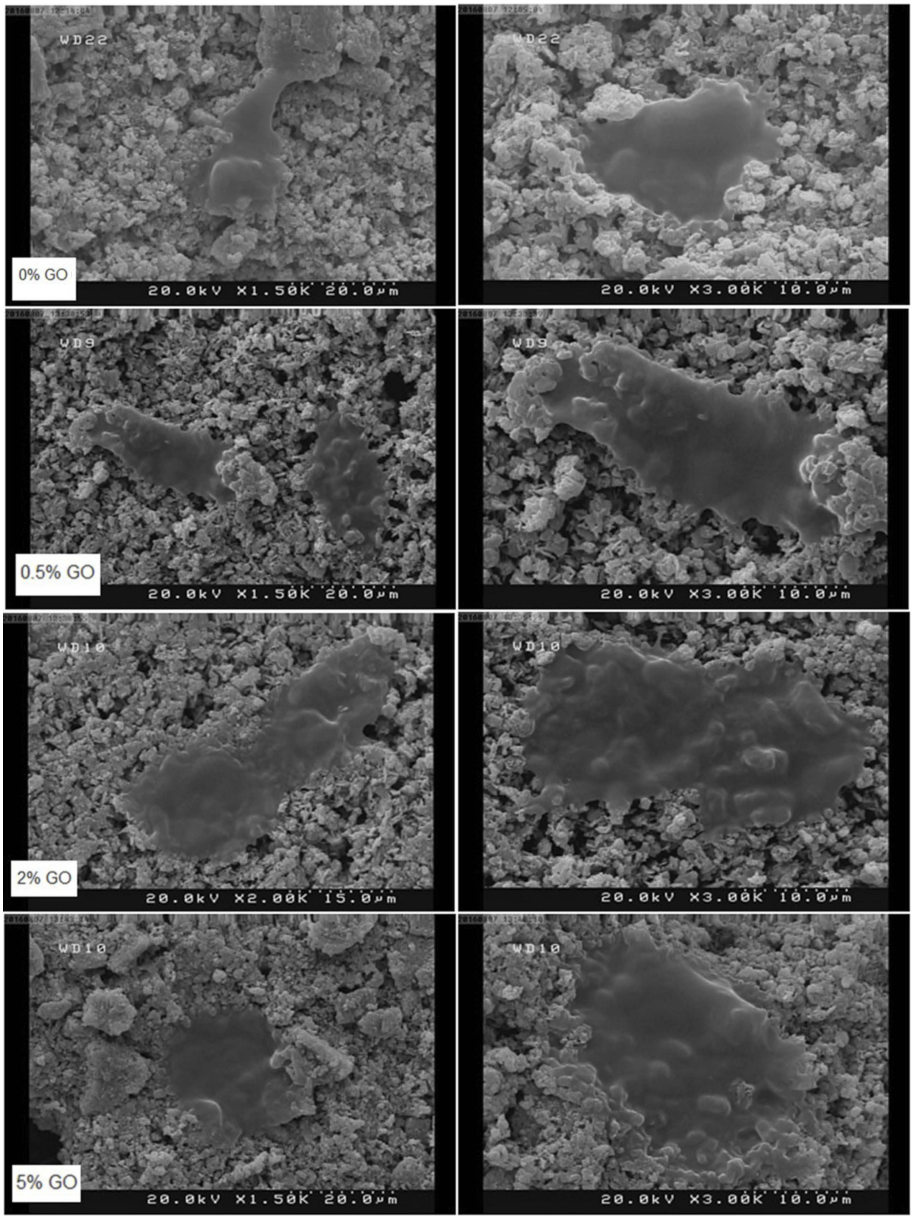

Figure 10 FESEM of cements cell attachment after 1 day.
Abbreviation: FESEM, Emission scanning electron microscopy.

ceramic exhibited worm-like crystals with the typical hydroxyapatite morphology.[11,25]

The FESEM micrographs revealed that more hydroxyapatite is formed on the surface of samples with more graphene oxide content. These results suggest that the incorporation of graphene oxide has not negatively influenced the formation of apatite on the CPC/GO composite.

Cell viability

Cell viability was studied by MTT assay. The OD values provide an indicator of the relative number of cells. Figure 9 presents the results assay for MG63 viability after 1, 3, and 7 days. The viability of the cells was decreased with increasing concentrations of graphene oxide. At higher concentrations, graphene oxide is considered to exhibit toxicity against cells.

On the other hand, graphene oxide at lower concentrations did not show any significant reduction in the cell viability compares with control samples. Moreover, by increasing the culture time to 7 days, there was a drop in the optical density. MTT results showed the dose-dependent cytotoxicity of graphene oxide. As the dose increased, the survival rate of cells decreased correspondingly.[15,26,27]

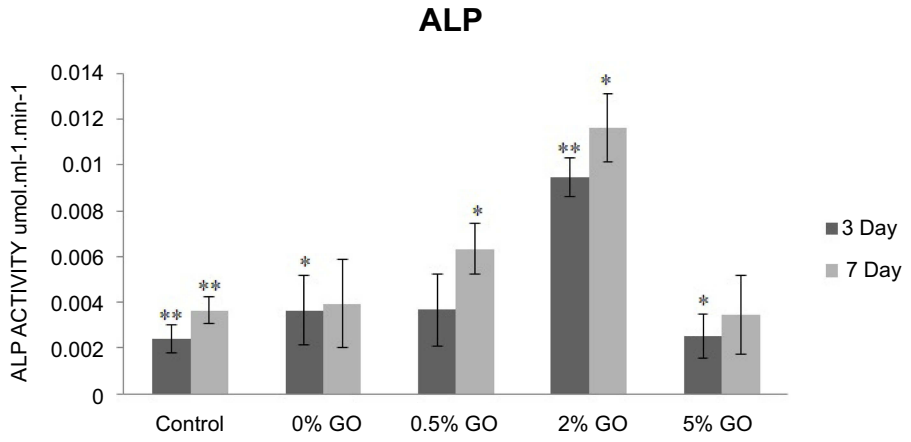

Figure 11 ALP activity of the MG63 cells cultured on specimens for 3 and 7 days.
Abbreviations: ALP, Alkaline phosphatase activity; GO, graphene oxide.

Cell attachment

Cell attachment to biomaterials depends not only on the surface morphology but also on the chemical composition of the biomaterial.[28] Poor cell attachment to the surface of brushite cement prepared with citric acid could be due to the presence of an intermediate phase that washed out during aging19 Figure 10 shows the MG63 attachment on aged samples after 24 h of culture. The cells were alive and spread on the all material's surface intimately. FESEM results confirmed that graphene oxide addition did not exhibit any obvious effects on cell attachment.

Alkaline phosphatase activity

ALP activity is an early marker of osteoblast differentiation.[29] Figure 11 shows the ALP activity of the MG63 cells cultured on specimens for 3 and 7 days. The ALP activity on the brushite cement with 2 wt.% graphene oxide is much higher than that of other samples. On day 3, ALP activity was equal for 0% and 0.5% CPC/GO samples. Activity at 7 days was decreased compared with that at 3 days. The experiment proves that the biocompatible CPC/GO composite provided a more effective substrate for cellular differentiation. It is possible that graphene oxide enhanced osteogenesis mineralization of the cells because of improving the nucleation of HA.[12]

Conclusion

The present study aims at investigating the suitability of GO/CPC composites as a bone filler. The XRD and FTIR spectrums indicated the successful synthesis of the β-TCP. In addition, XRD and AFM analyses confirmed the successful synthesis of graphene oxide. The composition properties of set cement also revealed the presence of calcium hydrogen diphosphate in 0%CPC/GO sample, but the pattern of 0.5% GO/CPC showed hydroxyapatite peaks. Mechanical testing of composite cement suggests that graphene oxide can increase the compressive strength of the cement. Other important properties such as setting time and porosity showed that results are well within the desired spans. The prepared composites induced in vitro cytotoxicity, depending on the concentration (up to 5% wt). According to the results of apatite mineralization in SBF, GO/CPC composites exhibit improved bioactivity as compared to the pure CPC. Moreover, the specimens could enhance the ALP activity of the composites. To conclude, the addition of GO seems to improve mechanical properties (GO<5%), but to induce only small improvements in cell activity and only with some specific GO percentages.

Availability of data and materials

The datasets used and/or analyzed during the current study available from the corresponding author on reasonable request.

Acknowledgments

We would like to thank from the "National Institute of Genetic Engineering and Biotechnology, Tehran" for their kind cooperation. The authors also gratefully acknowledge all the staff of Biotechnology Research Center, Shahrekord Branch, Islamic Azad University, Shahrekord in southwest Iran for their sincere support. The authors declare that no funding was received for the research.

Disclosure

The authors report no conflicts of interest in this work.

References

1. Nienhaus A, Hauptmann R, Fässler TF. ∞1[HgGe9]2- - a polymer with Zintl ions as building blocks covalently linked by heteroatoms. *Angew Chemie Int Ed*. 2002;41(17):3213–3215. doi:10.1002/1521-3773(20020902)41
2. Ginebra MP. Calcium phosphate bone cements. *Orthop Bone Cem*. 2008;206–230. doi:10.1533/9781845695170.2.206
3. Goldstein SA, Moalli MR. Current concepts in tissue engineering: cell, matrices, and genes. *Curr Opin Orthop*. 2001;12(5):424–427. doi:10.1097/00001433-200110000-00010
4. Zamanian A, Moztarzadeh F, Kordestani S, Hesaraki S, Tahriri M. Novel calcium hydroxide/nanohydroxyapatite composites for dental applications: in vitro study. *Adv Appl Ceram*. 2010;109(7):440–444. doi:10.1179/174367610X12804792635107
5. Roy M, Devoe K, Bandyopadhyay A, Bose S. Mechanical property and in vitro biocompatibility of brushite cement modified by polyethylene glycol. *Mater Sci Eng C*. 2012;32(8):2145–2152. doi:10.1016/j.msec.2012.05.020
6. Engstrand J, Persson C, Engqvist H. The effect of composition on mechanical properties of brushite cements. *J Mech Behav Biomed Mater*. 2014;29:81–90. doi:10.1016/j.jmbbm.2013.08.024
7. Zhao Y, Sun KN, Wang WL, et al. Microstructure and anisotropic mechanical properties of graphene nanoplatelet toughened biphasic calcium phosphate composite. *Ceram Int*. 2013;39(7):7627–7634. doi:10.1016/j.ceramint.2013.03.018
8. Zhang Z. Metal mediated cross-coupling reactions for carbon-carbon and carbon-nitrogen bonds formation under neutral pH conditions by accepted: Dean of the Graduate School. *Thesis*. 2011;5–8. doi:10.1002/smll
9. Ramanathan T, Abdala AA, Stankovich S, et al. Functionalized graphene sheets for polymer nanocomposites. *Nat Nanotechnol*. 2008;3(6):327–331. doi:10.1038/nnano.2008.96
10. Zhang L, Liu W, Yue C, et al. A tough graphene nanosheet/hydroxyapatite composite with improved in vitro biocompatibility. *Carbon N Y*. 2013;61:105–115. doi:10.1016/j.carbon.2013.04.074
11. Mehrali M, Moghaddam E, Shirazi SFS, et al. Synthesis, mechanical properties, and in vitro biocompatibility with osteoblasts of calcium silicate-reduced graphene oxide composites. *ACS Appl Mater Interfaces*. 2014;6(6):3947–3962. doi:10.1021/am500845x
12. Liu H, Cheng J, Chen F, et al. Gelatin functionalized graphene oxide for mineralization of hydroxyapatite: biomimetic and in vitro evaluation. *Nanoscale*. 2014;6(10):5315–5322. doi:10.1039/c4nr00355a
13. Li M, Wang Y, Liu Q, et al. In situ synthesis and biocompatibility of nano hydroxyapatite on pristine and chitosan functionalized graphene oxide. *J Mater Chem B*. 2013;1(4):475–484. doi:10.1039/c2tb00053a
14. Farzadi A, Solati-Hashjin M, Bakhshi F, Aminian A. Synthesis and characterization of hydroxyapatite/β-tricalcium phosphate nanocomposites using microwave irradiation. *Ceram Int*. 2011;37(1):65–71. doi:10.1016/j.ceramint.2010.08.021
15. Lim HN, Huang NM, Lim SS, Harrison I, Chia CH. Fabrication and characterization of graphene hydrogel via hydrothermal approach as a scaffold for preliminary study of cell growth. *Int J Nanomedicine*. 2011;6:1817–1823. doi:10.2147/IJN.S23392
16. Daculsi G, Ambrosio L. Development of a resorbable calcium phosphate cement with load bearing capacity. *Bioceram Dev Appl*. 2016;04:01. doi:10.4172/2090-5025.1000074
17. Unosson JE, Persson C, Engqvist H. An evaluation of methods to determine the porosity of calcium phosphate cements. *J Biomed Mater Res Part B Appl Biomater*. 2015;103(1):62–71. doi:10.1002/jbm.b.33173
18. Kokubo T, Takadama H. How useful is SBF in predicting in vivo bone bioactivity?. *Biomaterials*. 2006;27(15):2907–2915. doi:10.1016/j.biomaterials.2006.01.017
19. Jamshidi P, Bridson RH, Wright AJ, Grover LM. Brushite cement additives inhibit attachment to cell culture beads. *Biotechnol Bioeng*. 2013;110(5):1487–1494. doi:10.1002/bit.v110.5
20. Ghomash Pasand E, Nemati A, Solati-Hashjin M, Arzani K, Farzadi A. Microwave assisted synthesis & properties of nano HA-TCP biphasic calcium phosphate. *Int J Miner Metall Mater*. 2012;19(5):441–445. doi:10.1007/s12613-012-0576-4
21. Zhang L, Liang J, Huang Y, Ma Y, Wang Y, Chen Y. Letters to the editor size-controlled synthesis of graphene oxide sheets on a large scale using chemical exfoliation. *Carbon N Y*. 2009;47(14):3365–3368. doi:10.1016/j.carbon.2009.07.045
22. Ma R, Rafiee J, Wang Z, Song H, Yu Z, Koratkar N. Enhanced mechanical properties of nanocomposites at low graphene content. *ACS Nano*. 2009;3(12):3884–3890. doi:10.1021/nn9010472
23. Tamimi F, Sheikh Z, Barralet J. Dicalcium phosphate cements: brushite and monetite. *Acta Biomater*. 2012;8(2):474–487. doi:10.1016/j.actbio.2011.08.005
24. Baradaran S, Basirun WJ, Mahmoudian MR, Hamdi M, Alias Y. Synthesis and characterization of monetite prepared using a sonochemical method in a mixed solvent system of water/ethylene glycol/N,N-dimethylformamide. *Metall Mater Trans A Phys Metall Mater Sci*. 2013;44(5):2331–2338. doi:10.1007/s11661-012-1595-5
25. Zhong H, Wang L, Fan Y, et al. Mechanical properties and bioactivity of β-Ca2SiO4ceramics synthesized by spark plasma sintering. *Ceram Int*. 2011;37(7):2459–2465. doi:10.1016/j.ceramint.2011.03.037
26. Lee JH, Shin YC, Lee S, Jin OS, Kang SH. Enhanced osteogenesis by reduced graphene oxide/hydroxyapatite nanocomposites. *Nat Publ Gr*. 2015;1–13. doi:10.1038/srep18833
27. Zhang X, Hu W, Li J, Tao L, Wei Y. A comparative study of cellular uptake and cytotoxicity of multi-walled carbon nanotubes, graphene oxide, and nanodiamond. *Toxicol Res*. 2012;1:62. doi:10.1039/c2tx20006f
28. Chou SY, Cheng CM, LeDuc PR. Composite polymer systems with control of local substrate elasticity and their effect on cytoskeletal and morphological characteristics of adherent cells. *Biomaterials*. 2009;30(18):3136–3142. doi:10.1016/j.biomaterials.2009.02.037
29. Wang G, Zheng L, Zhao H, et al. *In vitro* assessment of the differentiation potential of bone marrow-derived mesenchymal stem cells on genipin-chitosan conjugation scaffold with surface hydroxyapatite nanostructure for bone tissue engineering. *Tissue Eng Part A*. 2011;17(9–10):1341–1349. doi:10.1089/ten.tea.2010.0497